

## A PROBABLISTIC FRAMEWORK USING A DISCRETE FE-BASED HOMOGENIZED MODEL FOR THE IN- AND OUT-OF-PLANE ANALYSIS OF MASONRY STRUCTURES

Luís C. Silva<sup>1</sup>, Gabriele Milani<sup>2</sup>, and Paulo B. Lourenço<sup>1</sup>

<sup>1</sup> ISISE University of Minho, Azurém 4800-058 Guimarães, Portugal  
address

e-mail: luisilva.civil@gmail.com; pbl@civil.uminho.pt

<sup>2</sup> Dept. of Architecture, Built environment and Construction engineering (A.B.C.), Technical Univer-  
sity in Milan, Piazza Leonardo da Vinci 32, 20133 Milan, Italy

e-mail: gabriele.milani@polimi.it

---

### Abstract

*Probabilistic-based type of analysis seems to constitute a state-of-art approach for earthquake engineers. Such strategy is, in the analysis of potential retrofitting measures for a building (or typology), needed for the development of vulnerability or fragility curves. This information is recognized to be extremely valuable within the decision process, since it allows the evaluation of the collapse probability (or other defined limit state) of a given structure under a given intensity measure.*

*The computational development integrated with the advent of proper working methodologies led to the increasing of research in the field. Nevertheless, the current numerical FE-based modelling approaches are still cumbersome for the dynamic analysis of the masonry behavior. In this scope, a novel stochastic methodology, based on the Latin Hypercube Sampling, using homogenization concepts for the masonry characterization and employing a discrete-FE based model is herein presented. Both running- and English-bond masonry textures are suitable to be studied, being the system uncertainty considered on parameters affecting the material, mechanical, geometrical and loading conditions.*

*The approach has been implemented on an English-bond masonry mockup tested on a shaking table in LNEC. An incremental dynamic analysis has been performed and fragility curves derived. It has been shown that the strategy is effective, accurate and very attractive from a computation point of view.*

**Keywords:** Masonry, Macro-model, Homogenization, Seismic vulnerability, LHS method.

---

## 1 INTRODUCTION

Performance-based earthquake engineering (PBEE) is a methodology in which a structure is designed to reach a desired performance state given a seismic excitation level [1, 2]. The first adoption of this philosophy dates from the Uniform Building Code ((PCBO) 1927) and current design guidelines still incorporate it as, for instance, the ASCE (2000) provides the maximum probability of a structure collapse according to the level of ground motion intensity. In the same line, Eurocode 8 (2004) sets the returning period of the seismic event to be considered conditioned by the type of class of the building, for both the non-collapse and damage limitation cases.

The 1994 M6.7 Northridge and 1995 M7.2 Hanshin-Awaji (Kobe) earthquakes showed that code-compliant design allows structures to behave well from a non-collapse requirement, but the damage control is hard to be assured leading to unacceptably high downtime and repair costs. Nonetheless, design codes feature a semi-probabilistic character, i.e. although the definition of the system variables is based on a simplified probabilistic estimation through safety factors, the final verification is purely deterministic because it relies on a ratio between the capacity and demand for each structural element. Such cut and dry approach does not guarantee the liability of engineers owing the uncertain nature of earthquakes.

Aiming a better control of the structural performance, reliability methods have been implemented within the PBEE frameworks; leading to the so-called second generation methods, as the PEER-PBEE developed by the Pacific Earthquake Engineering Research center (for further details see [6]). The PEER methodology introduced uncertainty in all the four stages of the seismic loss assessment: (1) hazard analysis (seismic action); (2) structural analysis; (3) damage analysis; and (4) decision analysis (consequences or loss). In this scope, the PEER-PBEE is the state-of-art framework for seismic loss assessment (already set in a technical standard designated as FEMA P-58 [7] and, therefore, it may serve as basis for application.

In this paper it is presented an alike framework applied for the seismic assessment of an URM structure. It is integrated with variables parametrization to account with probability-based concepts. Since it is computationally attractive, incremental dynamic analyses (IDA) are performed proving its applicability.

## 2 PROBABILISTIC NUMERICAL STRATEGY

Although the PBEE methodology is being disseminated through basic explanation [2], its multi-disciplinarily character, complexity and computational burden still precludes its use in common engineering practice. Bearing that the structural analysis stage represents a considerable amount of time, a novel probabilistic-based assessment structural analysis, which can be combined in such framework, is presented.

A two-step numerical procedure is introduced aiming to perform seismic vulnerability assessment studies for masonry structures. The strategy makes use of a classical first-order homogenization scheme and is so formed by: (i) the solution of the meso-scale problem; (ii) the meso-to-macro transition; and (iii) the solution of the macro-scale problem. The numerical framework relies on a direct homogenization approach, which involves solving a meso-mechanical problem at a meso-scale and deriving average field variables. This information is then carried out to the macro-scale to constitutively describe the behavior of the structure.

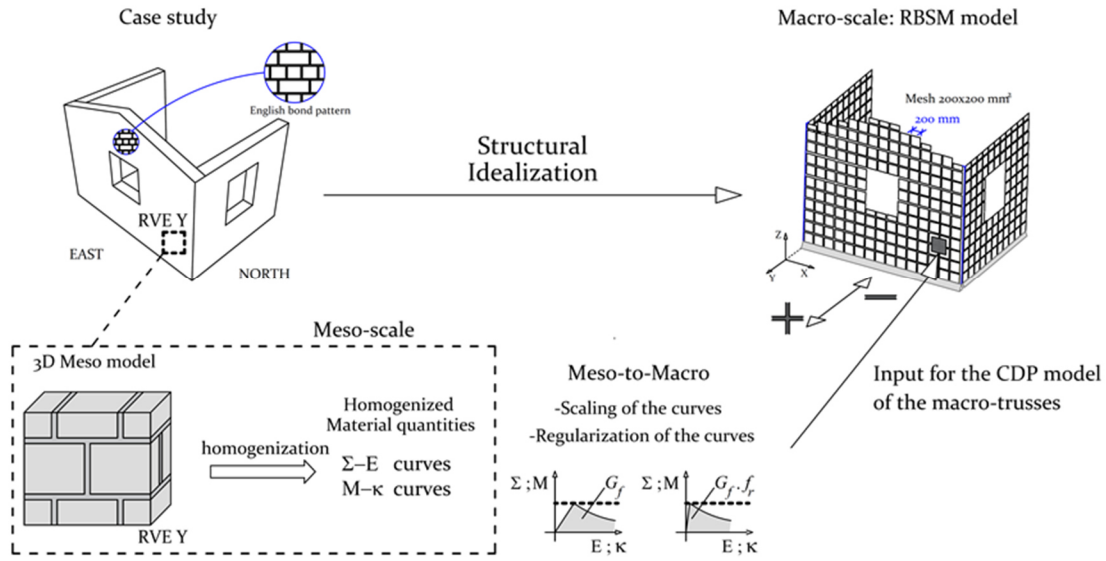


Figure 1: The methodology of the proposed two-step numerical procedure.

## 2.1 Meso-scale

Retrieving models at a meso-scale, which are both accurate and implementable on simplified two-step procedures is of most importance. Here, a three-dimensional meso-scale homogenized model is used to characterize the behavior of masonry at a cell level. The definition of a proper RVE is essential, once it may be statistically representative of the body under study. Here, the RVE definition follows the recommendations by Anthoine [8]. The use of such sophisticated approach, instead of a plate formulation, aims to guarantee that (i) the role of three-dimensional shear effects is accounted irrespective from the thickness value of the walls (as it has a major role as seen in [9]); and (ii) the presence of discontinuities in the thickness direction is accounted.

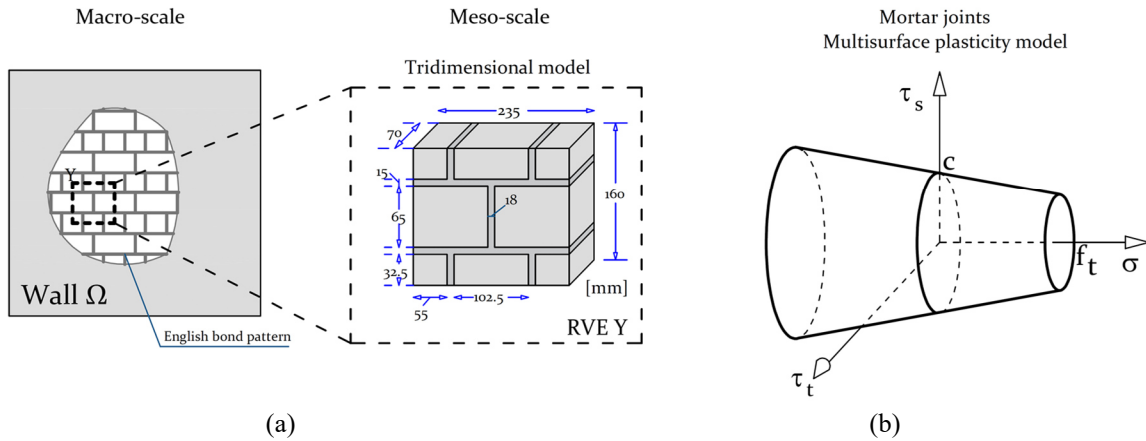


Figure 2: Meso-scale: (a) three-dimensional representative volume element (RVE) adopted; (b) multi-surface plasticity model adopted for mortar joints.

To decrease the computational demand, the material nonlinearity is assumed to be lumped on joints. This assumption seems to be adequate for strong block masonry structures. A multi-surface plasticity model, firstly developed by Lourenço et. al. [10] (the so-called composite interface model) and latter extended for three-dimensional interface elements by Van Zijl [11] is adopted. The plasticity models can reproduce well fracture, frictional slip and crushing along

the interface elements. The used strategy at a meso-scale has been already validated, see [9] for further details.

## 2.2 Macro-scale

The macro-structural behavior is represented through a discrete element model, designated as Rigid Body Spring Mass (RBSM), implemented in ABAQUS [12]. The discrete FE-method based procedure stems from the model presented by the authors in [13, 14] and represents both in- and out-of-plane deformation modes. The RBSM model, whose theoretical background is inspired in the works of Kawai (1978), is composed by the assemblage of discrete quadrilateral rigid plate elements interconnected, at its interfaces, through a set of rigid and deformable FE truss-beams, see Figure 3. The truss-beam elements govern both the deformation and damage of the structure, by being able to mimic the presence of the in- and out-of-plane failure modes considered in Figure 3 and within a decoupled characterization. These can append the material information of the meso-scale homogenized step and thus represent the masonry texture via an equivalent continuum media, by accounting with its orthotropy and full softening behavior description.

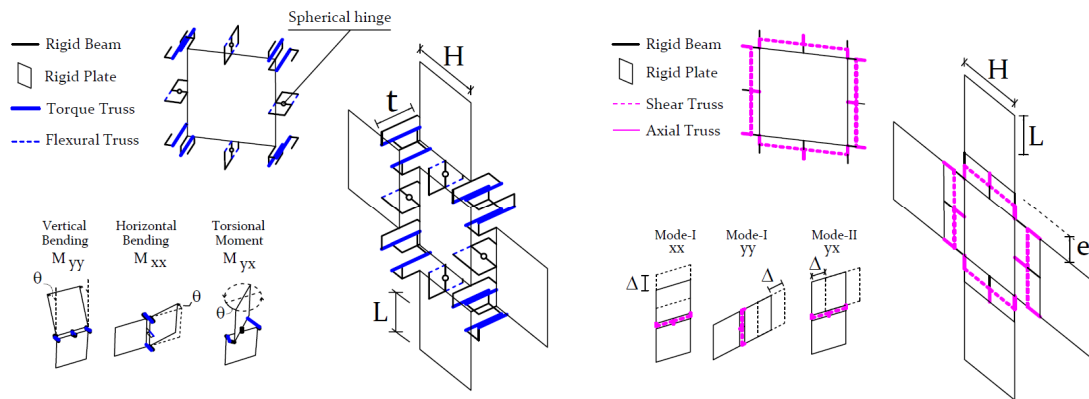


Figure 3: The Rigid-Body-Spring-Mass model adopted at a macro-scale.

Regarding the representation of the inertial forces, which highly affect the dynamic behaviour of a structure, the mass of the system shall be introduced. The mass of the system is embodied by the quadrilateral rigid plates using an equivalent material density which, following a linear displacement interpolation assumption, allows to achieve a consisted mass matrix. In this scope, the discrete element approach has been implemented into the commercial finite element software ABAQUS [12]. A Concrete damage plasticity (CDP) model was assumed for the representation of plasticity and damage. The damage is based on a scalar parameter  $d$  and the hysteretic behaviour given as depicted in Figure 4.

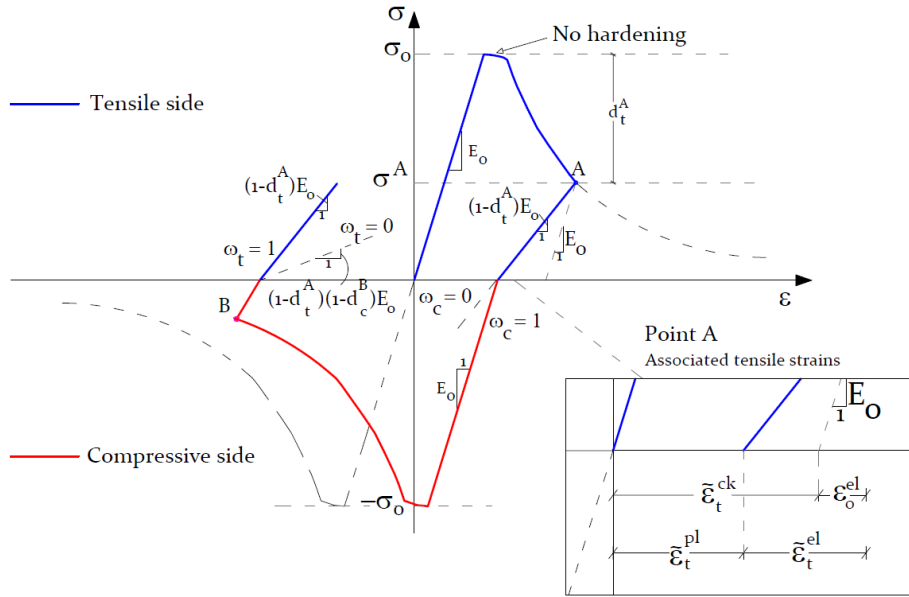


Figure 4: The hysteretic response of the macro-model for a generic input curve (valid for both in- and out-of-plane behaviors) using the CDP model.

### 2.3 Meso-to-macro

The CDP constitutive model demands the use of stress-strain relationships as input for the elements which govern the behaviour of the macro-model interfaces, i.e. the FE truss-beams. Bearing this, ad-hoc meso-to-macro transition steps are carried with the target of correcting the material input to be used by these interfaces in ABAQUS. Such transition is, however, only conducted after the structural modelling because it is dependent on the size of the used discrete mesh, particularly, from the values of  $H$ ,  $e$ ,  $L$ ,  $t$  (Figure 3). Furthermore, for the sake of simplicity, rectangular-square elements are assumed and so only two different angles are considered for the interfaces: 0 and 90 degrees. The material orthotropy is reproduced at a structural level because the approach offers the possibility to reproduce different input stress-strain relationships according to the trusses plane.

To what concerns with the in-plane behaviour, the stress quantities are directly derived from the macroscopic homogenized values. For the out-of-plane system, the macroscopic homogenized moment values are adapted to represent stress values for the bending and torsional truss beams through Eq. (1):

$$\sigma_{bending\ truss} = \frac{M}{(e.A_{BTruss})} \quad \sigma_{torque\ truss} = \frac{M}{(H.A_{TTruss})} \quad (1)$$

Here,  $M$  is the bending moment per unit of interface length,  $H$  the length of each quadrilateral panel,  $t$  is the thickness of the wall,  $A_{BTruss}$  is the bending truss area given by  $H(L + 0.5e)$  and  $A_{TTruss}$  is the torque truss area given by  $(eH)/2$ , where  $e$  (value of 20 mm) is the gap between the rigid plates, which ideally should be zero but in practice is assumed small enough to be able to place trusses between elements, and  $L$  is the influence length of each truss (equal to half of the mesh size, i.e.  $H/2$ ).

After the previous stage, the stress-strain curves are regularized by affecting the elastic stiffness and fracture energy terms. The regularization step is necessary to correctly identify the elastic stiffness of each truss beam and to guarantee the input independence of the macro-mesh and thus its objectivity in the nonlinear range. Through assuring the elastic energy equivalence, between the discrete model and a continuum homogeneous plate, it is possible to derive the

elastic stiffness of each truss-beam of the system. For the sake of conciseness, the demonstrations are disregarded.

The Elastic Young modulus of the in-plane axial trusses of a macro-unit cell for each plane direction (if orthotropy is considered) are derived and reads as:

$$E_{xx}^{in-plane\ axial\ truss} = \frac{\bar{E}_{xx}e}{4L+2e}; E_{yy}^{in-plane\ axial\ truss} = \frac{\bar{E}_{yy}e}{2(H+e)} \quad (2)$$

For the in-plane shear trusses, the elastic Young modulus is given by:

$$E_{xy}^{in-plane\ axial\ truss} = \frac{\bar{G}_{xy}H^2}{4e(2L+e)} \quad (3)$$

Regarding the out-of-plane behavior, the correct elastic Young Modulus of the out-of-plane flexural trusses is calculated according Eq. 4:

$$E_{ii}^{bending\ truss} = \frac{\bar{E}_{ii}t^4H}{24e(1-\nu^2)(H+e)eA_t} \quad (4)$$

For the torsional movement, the correct elastic Young modulus of the torque trusses is defined through Eq. 5.

$$E^{torsional\ truss} = \frac{2\bar{G}t^4}{3H^2e(2L+e)} \quad (5)$$

Where G is the shear modulus and calculated as  $\bar{G} = \frac{\bar{E}_{ii}}{2(1+\nu)}$ . By correcting the strain axis to calibrate the elastic stiffness value, the post-peak curve strains are also affected and so, in an implicit way, the fracture energy itself (the so-called regularization).

The methodology is briefly described in Figure 1 whereas the homogenized curves are transferred to a macro-scale. Two steps are developed to turn the macro-input independent from the macro-mesh i.e. the scaling and regularization of the homogenized quantities. The meso-scale model was developed in DIANA and a fully automatic procedure was achieved by exploiting the software programming capabilities [28]. This information is then carried out to the macro-scale to constitutively describe the behaviour of the structure.

### 3 APPLICATION

#### 3.1 Overview

The selected case study outcomes from the experimental works performed at LNEC by Candeias et al. [15]. Candeias et al. tested an unreinforced brick masonry structure composed by three walls in a U-shaped plan arrangement. The main façade (East plan) presents a gable wall and is linked with two transversal walls which act as abutments (North and South plans). These are constructed with a clay brickwork in an English-bond arrangement of 235 mm of thickness. The clay brick units have nominal dimensions of 235x115x70 mm<sup>3</sup> and are laid and bound together by mortar joints with a thickness ranging 15 to 18 mm. These geometrical features are represented in Figure 5.

The brick mock-up was tested up to collapse in a shaking table under a unidirectional seismic loading. The seismic input is applied in a perpendicular direction (E-W) to the main façade and derives from the strong ground motion component registered after the February 21 of 2011 earthquake occurred in Christchurch, New Zealand. Although only quasi-static analyses are developed, the numerical damage is compared with the observed experimental failure mechanisms.

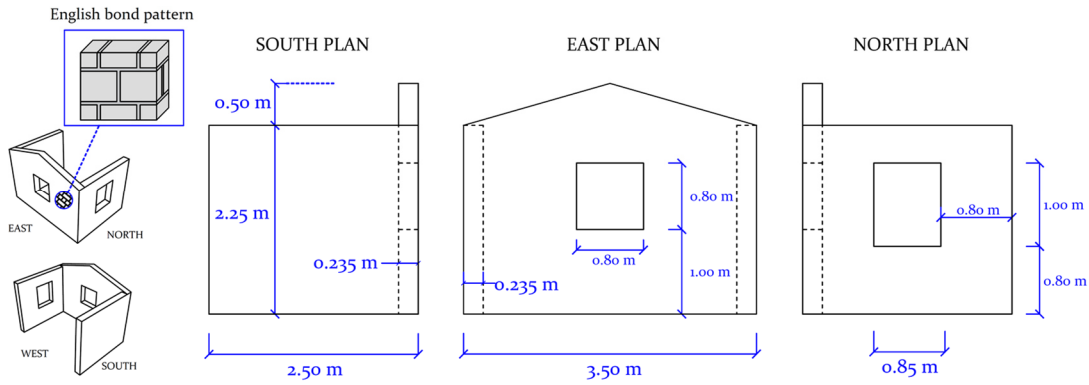


Figure 5: The geometry of the studied brick house mock-up (dimensions in meters) [27].

### 3.2 Random variables and correlation matrix

Uncertainties are commonly interpreted in engineering decision fields according to its origin and, therefore, differentiated as physical (in the sense of nature), statistical or modelling uncertainties [16]. The consideration of the latter is possible, within a structural-oriented problem, by defining the system variables as non-deterministic ones or, as typically designated in the literature, as random variables (RV's) [17, 18].

The set of random parameters which carry the uncertainty of the system can aggregate parameters from the loading input to the material and geometry of the structure. Complex methods allow to represent these RV's as, for instance, non-stationary stochastic processes [19, 20] although the definition of simple cumulative distribution functions and distribution parameters is sufficient in the majority of the structural problems. This fact is well addressed in the JCSS probabilistic model code [21], which puts together several valuable guidelines, rules, suggestions and/or explanations for a probabilistic-based structural design. Recommendations on the distribution functions and parameters values are presented for several construction materials as concrete, timber, and masonry thus serving to support the considerations gathered in Table 1.

Variables	Distribution	Mean	COV (%)
$\gamma$ (kN/m <sup>3</sup> )	Deterministic	1,890	3% [11]
$\nu$ (-)	Deterministic	0.25	-
$E_{\text{Brick}}$ (MPa)	Lognormal	11,000	30 % [11]
$E_{\text{Mortar}}$ (MPa)	Lognormal	3,000	25 % [18]
$f_{c,\text{mortar}}$ (MPa)	Lognormal	2.48	17 % [18]
$f_{t,\text{mortar}}$ (MPa)	Lognormal	0.105	*24 %
$G_{f,c}$ (N/mm)	Lognormal	3.97	*17 %
$G_f^I$ (N/mm)	Lognormal	0.012	*24 %
$G_f^{II}$ (N/mm)	Lognormal	0.05	*24 %
$c$ (N/mm)	Lognormal	0.2	40 % [18]
$\Phi$ (degrees)	Lognormal	30	19 % [18]
$t$ (mm)	Normal	235	5 % [11]
$t_{\text{joint}}$ (mm)	Normal	15	20 % [11]
$\xi$ (%)	Deterministic	3	-

Table 1: Set of system variables considered.

Selecting the proper  $n$ -dimensional array of random system variables  $X = \{X_1, X_2, X_3, \dots, X_n\}$  is, in a probabilistic-based numerical analysis, of most importance once it has a direct impact both in the necessary computational processing time and in the confidence level of the results. In a non-computational and time illimitation scenario, all the system variables should gather a level of uncertainty and, therefore, follow a probabilistic distribution. Mechanical, material and geometrical properties of the masonry are eligible to be random but, owing the reduction of the number of random variables, it has been decided that: (1) according to the low experimental variability registered in the selected case study, both the masonry density and Poisson coefficient are deterministic variables (see Table 1); (2) a tornado analysis should be conducted to support a rational decision of precluding any less relevant variable.

The results of the tornado diagrams from Figure 6 show that some parameters, as cohesion ( $c$ ), tensile strength ( $f_t$ ) and thickness ( $t$ ) unequivocally govern both the local (peaks) and global (energy) response of the homogenized  $\Sigma$ - $E$  and  $M$ - $\chi$  curves.

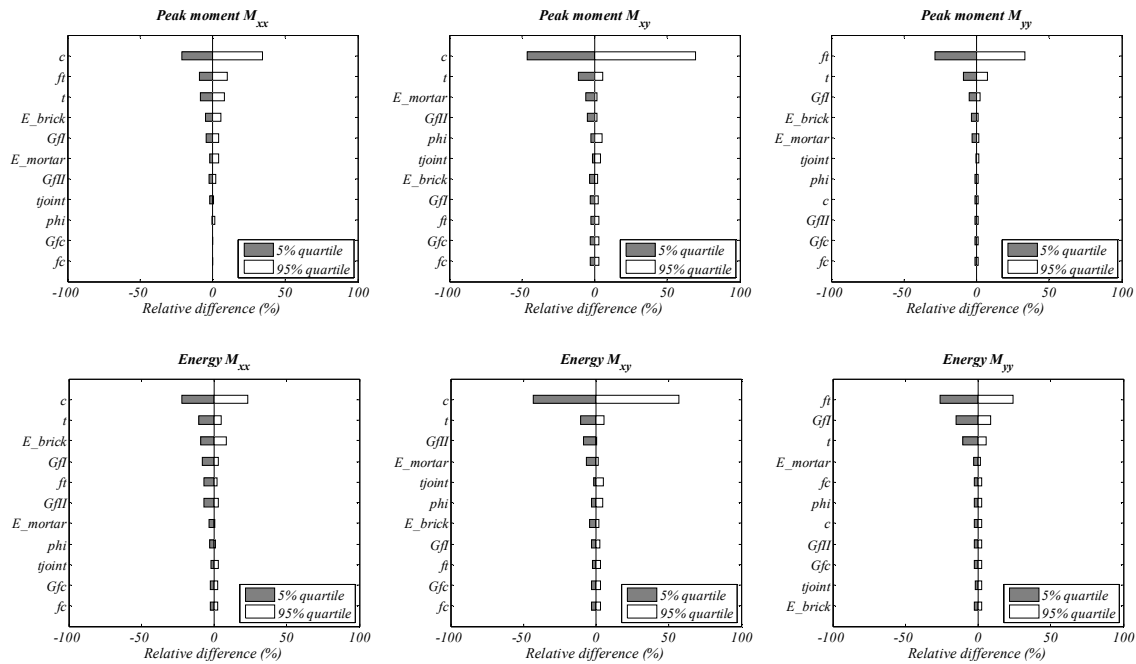


Figure 6: The tornado diagrams developed for the present case study.

On the other hand, it can be also addressed that the parameters concerning the compressive regime seem to have a lower effect. These results support the expert judgement and experimental evidences which states that, in the case of weak mortar masonry, the tensile and shear regimes tend to govern its overall behavior and, therefore, both the compressive strength and fracture energy can be deterministic with a marginal effect in the obtained results. So, a total of nine variables  $X_i$  are defined to be random and carry the aleatoric type of uncertainty:

$$X = (E_{brick}, E_{mortar}, f_t, G_f^I, c, G_f^{II}, \phi, t_{joint}, t)$$

### 3.3 Latin Hypercube Sampling

For simple problems, and when uncertainty is being considered, the failure probability can be evaluated solving the integral of the given limit state function [23]. For complex problems in a multi-dimensional space the determination of the latter solution is only achievable using probabilistic based methods, as the Monte Carlo (MC) or the Latin Hypercube (LH) [24].



These methods are widely spread in several engineering fields being the Monte Carlo (MC) approach developed first [25]. Both methods follow similar methodologies, i.e. the formulation of four main steps: (i) define a probability distribution type, and associated statistical parameters, for each random variable; (ii) generate a sample set of random variables, according to its distribution, potential correlation, and the number  $n$  of desired simulations; (iii) find the problems' solution by using each set of deterministic variables values; thus repeating the process  $n$  times; (iv) reach the failure probability through the ratio between the number of solutions which respect the limit function (or functions) and the total number  $n$  of simulations

The key difference between the MC and LH is the way that the sampling process is performed. Both suffer from a dimensionality curse, i.e. the more  $n$ s simulations are performed, the more correct is the solution. The former uses a simple random sampling method to define the set of random variables. The latter uses a stratified sampling technique, meaning that the existence of overlapped simulations is avoided [26]. In this context, LHS methods allow a lower computational effort [24] due to the rational selection of the random variables set.

For the problem at hand, the LHS method within an inverse transform method is chosen to assess the seismic vulnerability of the masonry case study. The sampling process intends to derive a set of grouped values, accounting with every admitted random variable, to possibly the estimation of the response variability under investigation. To enhance the representativity of the sample analysed, correlation has been considered, since the random parameters are generated according a Cholesky factorization of the covariance matrix of the random vector by LHS method according to the correlation coefficients.

$$\begin{bmatrix}
 & E_{brick} & E_{mortar} & f_t & G_f^I & c & G_f^{II} & f_c & t_{joint} & t \\
 E_{brick} & 1.0 & 0.4 & 0.2 & 0.2 & 0.2 & 0.2 & 0.2 & 0.0 & 0.0 \\
 E_{mortar} & & 1.0 & 0.8 & 0.6 & 0.6 & 0.4 & 0.2 & 0.0 & 0.0 \\
 f_t & & & 1.0 & 0.6 & 0.6 & 0.4 & 0.2 & 0.0 & 0.0 \\
 G_f^I & & & & 1.0 & 0.6 & 0.4 & 0.2 & 0.0 & 0.0 \\
 c & & & & & 1.0 & 0.6 & 0.2 & 0.0 & 0.0 \\
 G_f^{II} & & & & & & 1.0 & 0.2 & 0.0 & 0.0 \\
 f_c & & sym & & & & & 1.0 & 0.0 & 0.0 \\
 t_{joint} & & & & & & & & 1.0 & 0.2 \\
 t & & & & & & & & & 1.0
 \end{bmatrix} \quad (6)$$

In general, the following steps adopted: (1) define the set of random variables  $X = \{X_1, X_2, X_3, \dots, X_n\}$ ; (2) define the correlation matrix between the random variables; (3) develop the inverse transform method for each random variable; (4) Associate the random values to obtain a sample with  $n_s = 2000$  samples.

Figure 7 shows the obtained homogenized moment-curvature curves for  $M_{xx}$ ,  $M_{xy}$  and  $M_{yy}$  and the five representative curves derived (percentile 5% and 95%, quartile 25% and 75% and median). Notice that, since it has been seen that correlation exists between the latter curves for  $M_{xx}$ ,  $M_{xy}$  and  $M_{yy}$ , it is possible to attribute each one as a macro-model. In other words, five macro-models are obtained whose input is defined by the latter curves (also in terms of  $\Sigma$ -E curves).

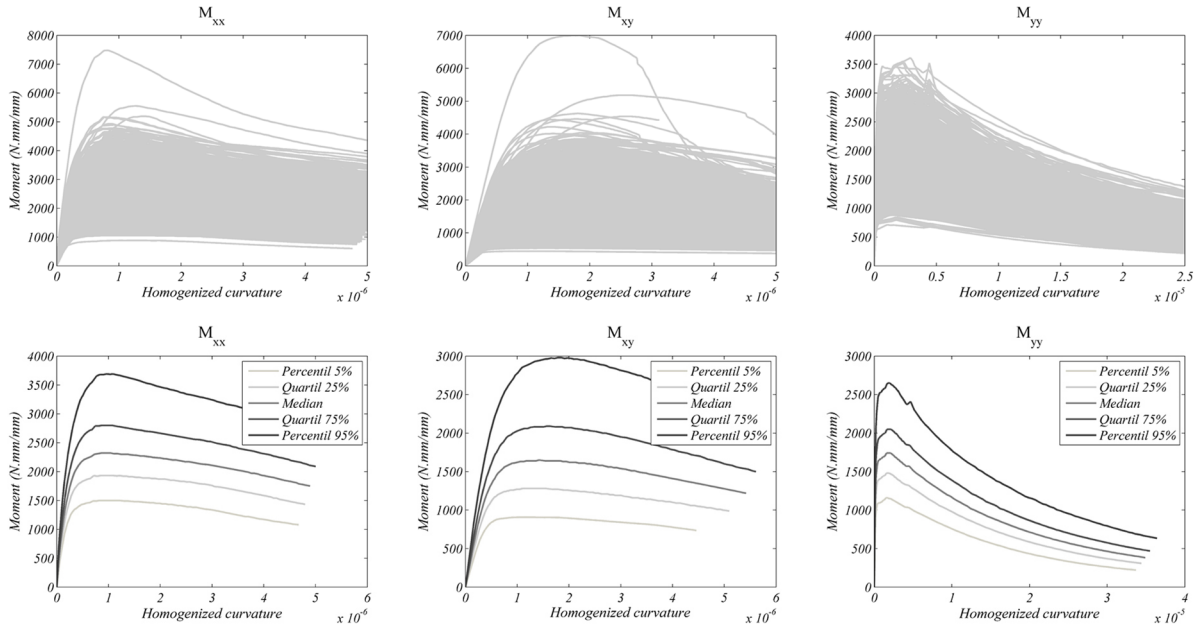


Figure 7: Homogenized moment-curvature curves obtained accounting with the derived LH sampling.

Figure 8 shows that the number of simulations adopted ( $n_s=2000$ ) seem to be adequate, once no significant variation is found in respect to the average of each peak  $M_{xx}$ ,  $M_{xy}$  and  $M_{yy}$  after  $n_s=1500$ .

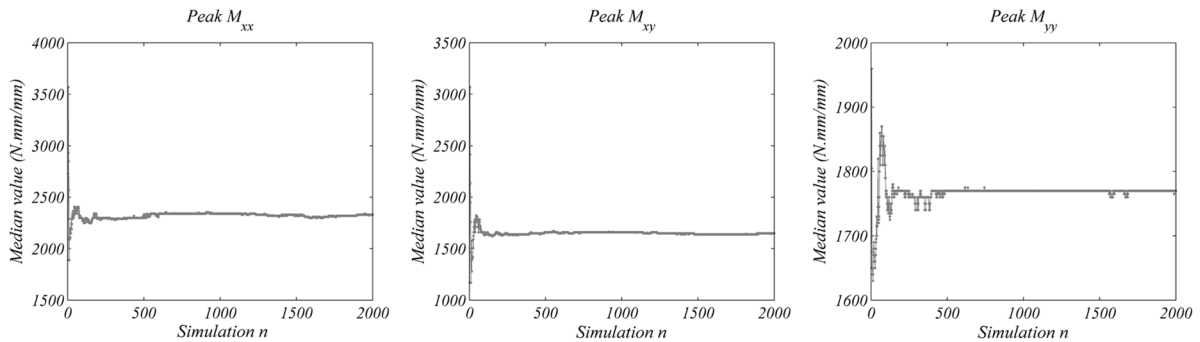


Figure 8: The mean value change of each random variable during the  $n$  simulations performed.

### 3.4 Incremental dynamic analysis (IDA)

Incremental dynamic analysis (IDA) is an intensive method which allows to give a better evaluation of the seismic response of a given structure. A series of scaled accelerograms are used to perform multiple nonlinear dynamic analyses [27, 28]. The construction of IDA curves demand the definition of (i) a proper set of ground motions and respective intensity measure (IM); and (ii) a proper engineering demand parameter (EDP).

Regarding the former, the current code guidelines (as [5]) acknowledge the use of real and artificial accelerograms. It is the earthquake engineer who should choice in conformity according to two key issues, the nature of application and the information at disposal. In regions where a significant set of ground motion records of damaging earthquakes is not available, the use of real earthquakes is difficult. Also, once each record has its own features in terms of wave characteristics contents (as frequency, duration, amplitude etc.) it is not expected that a similar seismic event occurs again. Bearing this, artificial accelerograms compatible with the elastic

response spectrum defined through design codes is used here. In fact, these are convenient once a significant number of random artificial motion records, compatible with the code design response spectrum, can be easily generated through existing tools. A total of 7 stationary signals have been here generated through the software SIMQKE\_GR [29], which is the minimum number according to the EC8 to be possible to consider the mean response.

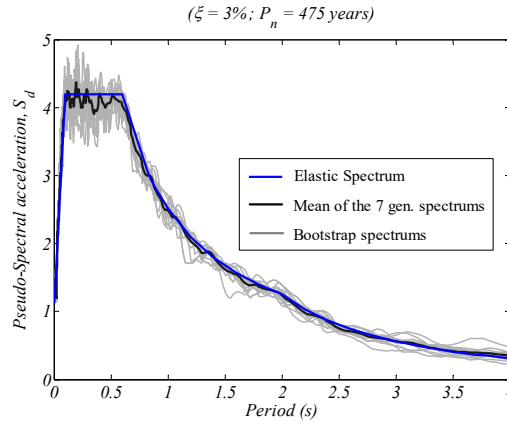


Figure 9: Pseudo-acceleration response spectrum: elastic spectrum according to EC8; response spectrum of the artificially generated earthquakes and mean spectrum of the 7 artificial earthquakes.

The non-stationary (in both amplitude and frequency content) signals are produced considering a trapezoidal shape for the envelope function [30] and have a duration with an intense phase of 30 seconds. The signals have been high-pass in the range of frequencies of 0.2 Hz to 40 Hz and filtered using a cosine function to attenuate potential accelerations drift. The resulting artificial accelerograms are compatible with the elastic response spectrum for an earthquake type 1 (far-fault earthquake) defined by EC8 [5] with a returning period of 475 years and for a 3% viscous damping ( $\xi = 3\%$ ) coefficient. The suggested parameters by the Portuguese National Annex for the region of Lisbon are followed for this study, as an importance factor  $\gamma_I$  equal to 1.0 (Class B buildings); a value of  $a_{gr} = 1.5 \text{ m/s}^2$ ; a soil type A (rock,  $S=1$ ). Note that the filtered signals presented in Fig.10 are scaled for the reference  $\text{PGA} = 1 \text{ g}$  ( $\text{m/s}^2$ ) and serve as reference. The intensity measure defined is the peak ground acceleration (PGA).

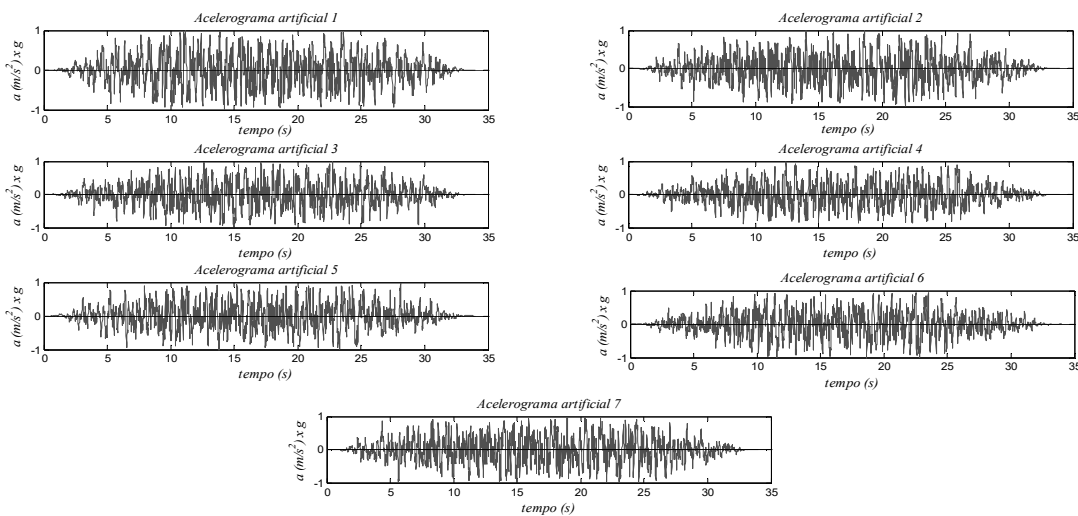


Figure 10: Artificial accelerograms generated to perform the IDA.

To what concerns the engineering demand parameter (EDP), it has been considered that the demand is given by the maximum out-of-plane displacement obtained at the top of the gable wall, see Figure 11. A displacement-based parameter is typically adopted for the masonry structures, as [28]. The IDA curves obtained for each of the defined five macro-models, which represent 2000 samples with a total of nine random parameters, (including both material and geometrical) are depicted in Figure 11. It is possible to conclude that, for the percentile 5%, quartile 25% and median models, the structure shows a steep increase of the displacements after a PGA of  $0.4\text{m/s}^2$ . On the other hand, the two models which have higher strength values (quartile 75% and percentile 95%) do not present any significant difference on the displacements found.

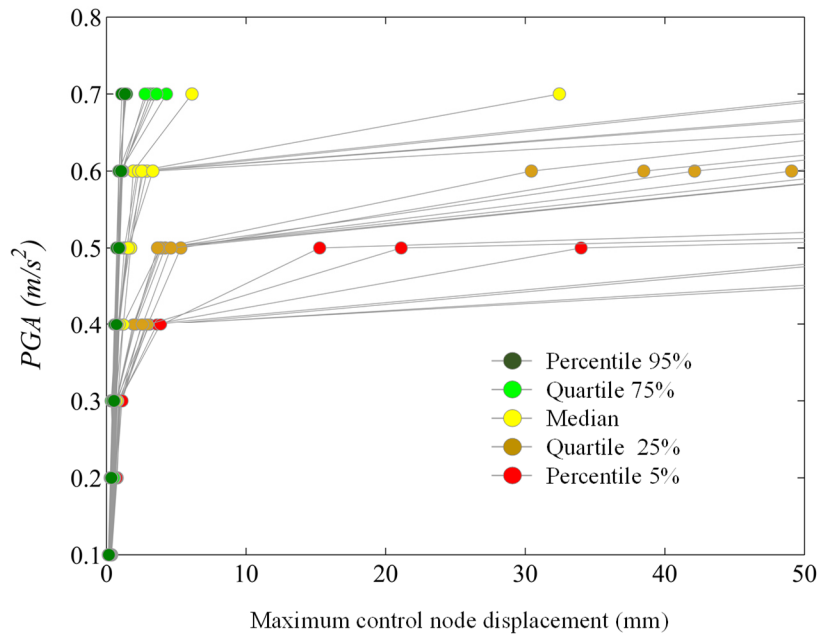


Figure 11: IDA curves obtained for the five macro-models (7 earthquakes).

#### 4 CONCLUSIONS

A two-step framework aiming the study of the dynamic response of a masonry structure has been presented. It is able to account with the system uncertainties. The strategy was previously validated in the quasi-static and dynamic ranges, being the enclosed novelty the parametrization of the input variables in order to feature a probabilistic nature. This uses a homogenization approach to characterize the random behaviour of the material at a meso-scale. At a macro-scale, the masonry structures are represented through a discrete FE model which includes the data obtained from the foregoing scale, namely the homogenized  $\Sigma$ -E and M- $\chi$  curves. The strategy allows the processing of dynamic analyses within an attractive computational time. In this scope, a Latin Hypercube method was used to derive 2000 samples. Each sample corresponds to a set of seven mechanical and two geometrical parameters (thickness of the wall and thickness of the masonry joints). At a macro-scale and considering the statistical variability of the homogenized data, five representative models were defined. Incremental dynamic analyses (IDA) were performed, where the out-of-plane displacement is the demand parameter and the PGA the intensity measure (seven earthquakes from  $0.1$ - $0.7\text{m/s}^2$ ). The 245 IDA curves showed a high response variability of the case study. It seems clear that PGA values higher than  $0.4\text{m/s}^2$  lead to a steep increase of the observed displacements.

At last, it may be noted that the probabilistic-based framework was successfully implemented. It can be integrated within a seismic vulnerability assessment of masonry structures if proper damage limits are accounted; or within a seismic loss estimation study if, additionally, consequence costs are included.

## REFERENCES

- [1] A. Ghobarah, "Performance-based design in earthquake engineering: state of development," *Eng. Struct.*, vol. 23, no. 8, pp. 878–884, 2001.
- [2] S. Günay and K. M. Mosalam, "PEER Performance-Based Earthquake Engineering Methodology, Revisited," *J. Earthq. Eng.*, vol. 17, no. 6, pp. 829–858, Aug. 2013.
- [3] Pacific Coast Building Officials (PCBO), *Uniform Building Code*. Whittier, California, 1927.
- [4] American Society of Civil Engineers (ASCE), *Prestandard and Commentary for the seismic Rehabilitation of Buildings*. Washington, DC, USA, 2000.
- [5] Eurocode 8, "Eurocode 8. Design provisions for earthquake resistance of structures. Part 1-1: General rules – seismic actions and general requirements for structures.," Brussels, Belgium Eur. Committee Stand., 2004.
- [6] K.A. Porter, "An overview of PEER's performance-based earthquake engineering methodology," in *Ninth International Conference on Applications of Statistics and Probability in Engineering*, 2003.
- [7] Applied Technology Council (ATC), *FEMA P-58: Seismic Performance Assessment of Buildings*. Washington, DC, USA: Federal Emergency Management Agency, 2012.
- [8] A. Anthoine, "Derivation of the in-plane elastic characteristics of masonry through homogenization theory," *Int. J. Solids Struct.*, vol. 32, no. 2, pp. 137–163, Jan. 1995.
- [9] L. C. Silva, P. B. Lourenço, and G. Milani, "Derivation of the out-of-plane behaviour of masonry through homogenization strategies: micro-scale level," *Comput. Struct.*, vol. 209, pp. 30–43, 2018.
- [10] P. B. Lourenço and J. G. Rots, "Multisurface Interface Model for Analysis of Masonry Structures," *J. Eng. Mech.*, vol. 123, no. 7, pp. 660–668, Jul. 1997.
- [11] G. P. A. G. Zijl, "Computational Modelling of Masonry Creep and Shrinkage," Delft University of Technology, 2000.
- [12] ABAQUS, "Finite Element Analysis (Theory manual)," RI: Dassault Systèmes Simulia Corporation, Providence, Release 6.6 (software), 2013.
- [13] L. C. Silva, P. B. Lourenço, and G. Milani, "Rigid block and spring homogenized model (HRBSM) for masonry subjected to impact and blast loading," *Int. J. Impact Eng.*, vol. 109, pp. 14–28, 2017.
- [14] L. C. Silva, P. B. Lourenço, and G. Milani, "Nonlinear Discrete Homogenized Model for Out-of-Plane Loaded Masonry Walls," *J. Struct. Eng.*, vol. 143, no. 9, Sep. 2017.
- [15] P. X. Candeias, A. C. Costa, N. Mendes, A. A. Costa, and P. B. Lourenço, "Experimental Assessment of the Out-of-Plane Performance of Masonry Buildings Through Shaking Table Tests," *Int. J. Archit. Herit.*, pp. 1–28, Dec. 2016.

- [16] A. S. Nowak and K. Collins, R., *Reliability of Structures*, Second. CRC Press, Taylor & Francis Group, 2012.
- [17] M. H. Faber, M. A. Maes, J. W. Baker, T. Vrouwenvelder, and T. Takada, "Principles of risk assessment of engineered systems," in *10th International Conference on Applications of Statistics and Probability in Civil Engineering*, 2007.
- [18] M. H. Faber and M. G. Stewart, "Risk assessment for civil engineering facilities: critical overview and discussion," *Reliab. Eng. Syst. Saf.*, vol. 80, no. 2, pp. 173–184, May 2003.
- [19] M. G. Stewart and R. E. Melchers, *Probabilistic Risk Assessment of Engineering Systems*. ITP, 1997.
- [20] R. E. Melchers, *Structural Reliability Analysis and Prediction*, Second. Wiley, 1999.
- [21] JCSS, "Joint Committee on Structural Safety - Probabilistic Model Code PART 3: Resistance Models," 3.2, 2011.
- [22] JCSS, "Joint Committee on Structural Safety - Probabilistic Model Code PART 3: Resistance Models," 3.2, 2011.
- [23] P. D. M. H. Faber, *Risk and Safety in Engineering*. Zurich: Swiss Federal Institute of Technology, 2009.
- [24] M. Stein, "Large Sample Properties of Simulations Using Latin Hypercube Sampling," *Technometrics*, vol. 29, no. 2, pp. 143–151, 1987.
- [25] N. Metropolis and S. Ulam, "The Monte Carlo Method," *J. Am. Stat. Assoc.*, vol. 44, no. 247, pp. 335–341, 1949.
- [26] M. D. McKay, R. J. Beckman, and W. J. Conover, "Comparison of Three Methods for Selecting Values of Input Variables in the Analysis of Output from a Computer Code," *Technometrics*, vol. 21, no. 2, pp. 239–245, 1979.
- [27] D. Vamvatsikos and C. A. Cornell, "Incremental dynamic analysis," *Earthq. Eng. Struct. Dyn.*, vol. 31, no. 3, pp. 491–514, Mar. 2002.
- [28] D. Vamvatsikos and M. Fragiadakis, "Incremental dynamic analysis for estimating seismic performance sensitivity and uncertainty," *Earthq. Eng. Struct. Dyn.*, vol. 39, no. 2, pp. 141–163, Feb. 2010.
- [29] P. Gelfi, "SIMQKE-GR - Software for generating artificial accelerograms compatible with the response spectrum." University of Brscia, Italy, 2006.
- [30] D. A. Gasparini and E. H. Vanmarke, "Simulated earthquake motions compatible with prescribed response spectra. Evaluation of Seismic Safety of Buildings," Report no 2, 1976.